Biomedicine & Pharmacotherapy 144 (2021) 112326

Contents lists available at ScienceDirect

Biomedicine & Pharmacotherapy

journal homepage: www.elsevier.com/locate/biopha

Immunosuppressant flavonoids from *Scutellaria baicalensis*

Nova Syafni [a,b], Seema Devi [c], Amy M. Zimmermann-Klemd [c], Jakob K. Reinhardt [a], Ombeline Danton [a], Carsten Gründemann [d], Matthias Hamburger [a,*]

[a] Pharmaceutical Biology, Department of Pharmaceutical Sciences, University of Basel, Basel, Switzerland
[b] Faculty of Pharmacy and Sumatran Biota Laboratory, University of Andalas, Padang, West Sumatra, Indonesia
[c] Center for Complementary Medicine, Institute for Infection Prevention and Hospital Epidemiology, Faculty of Medicine, University of Freiburg, Freiburg, Germany
[d] Translational Complementary Medicine, Department of Pharmaceutical Sciences, University of Basel, Basel, Switzerland

ARTICLE INFO

Keywords:
Scutellaria baicalensis
T-lymphocyte proliferation
Immunosuppressant activity
HPLC based activity profiling
Flavonoids

ABSTRACT

Some plants used in Traditional Chinese Medicine serve as treatment for disease states where a suppression of the cellular immune response is desired. However, the compounds responsible for the immunosuppressant effects of these plants are not necessarily known.

The immunosuppressant compounds in the roots of *Scutellaria baicalensis*, one of the most promising plants identified in a previous screening, were tracked by HPLC activity profiling and concomitant on-line spectroscopic analysis. Compounds were then isolated by preparative chromatography, and structures elucidated by spectroscopic methods. Twelve flavonoids (**5–16**) were identified from the active time windows, and structurally related flavones **2**, **4**, and **17**, and flavanones **1** and **3** were isolated from adjacent fractions. All flavonoids possessed an unusual substitution pattern on the B-ring, with an absence of substituents at C-3 and C-4. Compounds **11**, **13**, **14**, and **16** inhibited T-cell proliferation (IC_{50} values at 12.1–39 μM) at non-cytotoxic concentrations. The findings may support the use of *S. baicalensis* in disorders where a modulation of the cellular immune response is desirable.

1. Introduction

The immune system is built to discriminate self from non-self antigens. The loss of immunological tolerance to antigens can produce autoreactive immune responses [1]. Immunosuppressive agents are an option for treating this condition. Since T-lymphocytes are a self-centered network in the immune system, most immunosuppressant drugs target the mechanism of enormous diversity in T-cells receptor and signaling pathways. An over-stimulated CD28 pathway (costimulatory pathways in T-cells) causes excessive proliferation and differentiation of naïve T-cells. The dysfunction of these costimulatory pathways triggers autoimmune diseases such as type-I diabetes and rheumatoid arthritis [2].

We recently screened an extract library prepared from 435 traditional Chinese herbal drugs for their ability to inhibit T-cell proliferation without concomitant cytotoxicity [3,4]. One of the promising hits in this screening was a dichloromethane (DCM) extract from roots of *Scutellaria baicalensis* Georgi (Lamiaceae) which exhibited an IC_{50} of 12.9 μg/mL. Huang Qin (黄芩; Scutellariae baicalensis radix) is a widely used herbal drug in Traditional Chinese Medicine, and monographs have been published in the Chinese Pharmacopoeia (2015), the European Pharmacopoeia (EP 9.0), the British Pharmacopoeia (BP 2018), and the United States Pharmacopeia (USP 2020). The drug has been traditionally used for the treatment of nausea and vomiting in febrile diseases, dysentery, epistaxis, hemorrhage, inflammation, and respiratory infections [5]. Flavonoids are the major secondary metabolites in the roots, and flavone glycosides (wogonin glucoside, baicalin, oroxyloside) and their aglycones (wogonin, baicalein, oroxyloside) have been identified [6]. We here report on the activity-driven identification of compounds responsible for the immunosuppressant activity of the extract, and on the further evaluation of their activity.

* Corresponding author.
E-mail addresses: nova.syafni@unibas.ch (N. Syafni), seema.devi@uniklinik-freiburg.de (S. Devi), amy.klemd@uniklinik-freiburg.de (A.M. Zimmermann-Klemd), jakob.reinhardt@unibas.ch (J.K. Reinhardt), ombeline.danton@unibas.ch (O. Danton), carsten.gruendemann@unibas.ch (C. Gründemann), matthias.hamburger@unibas.ch (M. Hamburger).

https://doi.org/10.1016/j.biopha.2021.112326
Received 5 August 2021; Received in revised form 6 October 2021; Accepted 8 October 2021
Available online 13 October 2021

2. Materials and methods

2.1. General

HPLC-grade acetonitrile (Scharlau) and water (Barnstead EASY-pure II water purification system) were used for HPLC separations. For analytical separations HPLC solvents contained 0.1% formic acid (Scharlau). DMSO (Scharlau) was used for dissolving the samples for HPLC analysis. Solvents used for extraction, column chromatography, and recrystallization were of technical grade (Romil Pure Chemistry) and were redistilled before use. Silica gel 60 F_{254} coated aluminum TLC plates and silica gel (0.063–0.200 mm) for column chromatography were from Merck. TLC plates were visualized under UV light and by spraying with 1% vanillin (Roth) in EtOH, followed by 10% sulfuric acid (Scharlab) in EtOH and heating at 110 °C. Reagent grade aluminium chloride (Sigma-Aldrich) and reagent grade 36% hydrochloric acid (Hänseler) were used to prepare UV/Vis shift reagents. HPLC-grade methanol (Scharlau) was used for UV, optical rotation and ECD measurements. Deuterated solvent (DMSO-d_6) for NMR was purchased from Armar Chemicals. Evaporation of microfractions was done with a Genevac® EZ-2 plus vacuum centrifuge (Avantec).

HPLC-PDA-ELSD-MS analyses and HPLC-based microfractionation were performed with an instrument consisting of a degasser, quaternary pump (LC-20 CE), column oven (CTO-20AC), PDA detector (SPD-M20A), and triple quadrupole mass spectrometer (LCMS-8030) (all Shimadzu), connected via a T-split to an ELSD 3300 detector (Alltech). A SunFire® C18 column (3.5 μm, 3.0 × 150 mm) equipped with a guard column (3.0 ×10 mm) (Waters) was used for analytical separations. Data acquisition and processing were performed using lab solution software (Shimadzu).

Flash chromatography was carried out on a Puriflash® 4100 system (Interchim). A glass column (25 ×460 mm i.d.) was used. Semi-preparative HPLC was carried out with an Agilent 1100 Series instrument with a PDA detector, and with a Waters 2690 instrument consisting of a degasser, binary high pressure mixing pump, column oven, and a Waters 996 photodiode array detector. A SunFire® Prep C18 column (5 μm, 10 ×150 mm) equipped with a guard column (10 ×10 mm) (Waters) was used for separation.

NMR spectra were recorded with a Bruker Avance® III spectrometer operating at 500.13 MHz for ^{1}H and 125.77 MHz for ^{13}C. ^{1}H NMR experiments and 2D homonuclear and heteronuclear NMR spectra were measured with a 1 mm TXI probe at 18 °C. ^{13}C NMR spectra were obtained in 3 or 5 mm tubes with a BBO probe at 23 °C. Data were analyzed using ACD/Spectrus Processor 2017.1.3.

Optical rotations were measured in MeOH on a P-2000 digital polarimeter (Jasco) equipped with a sodium lamp (589 nm) and a 10 cm temperature-controlled microcell. Electronic circular dichroism (ECD) spectra were recorded, at a concentration of 0.1 mg/mL in MeOH, on a Chirascan CD spectrometer with 1 mm path precision cells (110 QS, Hellma Analytics). UV/Vis absorption spectra were recorded with a Lambda 35 spectrometer (PerkinElmer), either in pure MeOH and after addition of $AlCl_3$/HCl [7].

2.2. Plant material

Dried roots of *Scutellaria baicalensis* Georgi (Scutellariae baicalensis radix EP 9) were purchased in November 2017 from Lian Chinaherb (Wollerau, Switzerland), lot number S1310444C. A voucher specimen has been deposited at the Division of Pharmaceutical Biology, University of Basel, under plant number 1020.

2.3. Microfractionation for activity profiling

For microfractionation of the extract an FC 204 fraction collector (Gilson) adapted for 96-deepwell plates was connected to the LC-MS 8030 system (Shimadzu). Three injections of the extract (10 mg/mL in DMSO) were carried out: 2 × 30 μL (corresponding in total to 0.6 mg of extract) with only the PDA detector for collection of microfractions, and 1 × 10 μL with PDA-ELSD-ESI-MS detection for recording of on-line spectroscopic data. Water with 0.1% formic acid (A) and acetonitrile with 0.1% formic acid (B) were used as mobile phase. The gradient was 20–100% B in 30 min, followed by 10 min at 100% B. Microfractions of 1 min each were collected from minute 2 to minute 35, whereby corresponding microfractions of the two runs were collected into the same well. The deepwell plate was dried in a Genevac EZ-2 evaporator, and residues re-dissolved in DMSO prior to the bioassay.

2.4. Extraction and isolation

Powdered *S. baicalensis* roots (160 g) were extracted at room temperature and under stirring with 2 × 400 mL DCM for two days each. The combined extracts were evaporated under reduced pressure to afford 1.4 g of dry residue. The extract was chromatographed on a silica gel column (25 ×460 mm) at a flow rate of 25 mL/min, using a step gradient (*n*-hexane, *n*-hexane/EtOAc, EtOAc, EtOAc/MeOH and MeOH). A total of 35 fractions were collected. Compounds detected in the active time window of the HPLC activity profile were localized in fractions 10, 13, 16, 18, 21, and 26, respectively. These fractions were further purified by semi-preparative HPLC and recrystallization.

Compound **11** (26.0 mg) was obtained from fraction 16 (47.2 mg) via recrystallization from a methanol/ethanol mixture. Fraction 10 (31.4 mg) was separated by semi-preparative RP-HPLC [H_2O + 0.1% formic acid (A), MeCN + 0.1% formic acid (B); 44% B (0–20 min); flow rate 4 mL/min] to afford **16** (17.0 mg, t_R 15.1 min). Fraction 13 (8.5 mg) (semi-preparative RP-HPLC [H_2O + 0.1% formic acid (A), MeCN + 0.1% formic acid (B); isocratic 42% B (0–25 min); flow rate 4 mL/min]) afforded compound **13** (2.1 mg, t_R 14.1 min), and fraction 18 (16.0 mg) [H_2O + 0.1% formic acid (A), MeCN + 0.1% formic acid (B); 43–45% B (0–25 min); flow rate 4 mL/min] yielded compounds **11** (1.6 mg, t_R 12.0 min), **12** (3.5 mg, t_R 12.5 min), **15** (5.8 mg, t_R 13.5 min), and **17** (5.4 mg, t_R 15.6 min). Fraction 21 (70.4 mg) (semi-preparative RP-HPLC [H_2O + 0.1% formic acid (A), MeCN + 0.1% formic acid (B); 38–42% B (0–25 min); flow rate 4 mL/min]) yielded compounds **10** (6.0 mg, t_R 14.9 min), and **14** (50.0 mg, t_R 18.2 min), fraction 26 (25.5 mg) [H_2O + 0.1% formic acid (A), MeCN + 0.1% formic acid (B); 38–42% B (0–25 min); flow rate 4 mL/min] afforded compounds **3** (1.1 mg, t_R 12.9 min), **4** (0.6 mg, t_R 17.9 min), **5** (1.3 mg, t_R 21.3 min), **8** (3.4 mg, t_R 24.3 min), **6** (0.3 mg, t_R 26.1 min), **7** (0.2 mg, t_R 27.4 min), and **9** (1.0 mg, t_R 28.0 min), and fraction 29 (17.5 mg) [H_2O + 0.1% formic acid (A), MeCN + 0.1% formic acid (B); 21–24% B (0–24 min); flow rate 4 mL/min] gave compounds **1** (0.5 mg, t_R 9.1 min) and **2** (1.0 mg, t_R 19.1 min).

(2 S)− 7,2′,6′-Trihydroxy-5-methoxyflavanone (**1**): yellowish amorphous solid, $[\alpha]_D^{25}$ = 11.2 (*c* 0.03, MeOH); ECD (MeOH, *c* 0.1 mg/mL, 1 mm path length)) λ_{max} (Δε): 223 (+3.5), 278 (−1.3), 332 (+0.9); ^{1}H and ^{13}C NMR, see Table S1, Supplementary Material; ESIMS *m/z* 303 $[M+H]^+$.

5,7,3′,6′-Tetrahydroxy-8,2′-dimethoxyflavone (Viscidulin III) (**2**): pale yellow amorphous solid, ^{1}H and ^{13}C NMR, see Table S2, Supplementary Material; ESIMS *m/z* 347 $[M+H]^+$.

(2 S)− 5,7,2′,6′-Tetrahydroxyflavanone (**3**): yellowish amorphous solid, $[\alpha]_D^{25}$ = 20.7 (*c* 0.02, MeOH); ECD (MeOH, *c* 0.2 mg/mL, 1 mm path length)) λ_{max} (Δε): 223 (+2.9), 284 (−1.9), 325 (+0.5); ^{1}H and ^{13}C NMR, see Table S1, Supplementary Material; ESIMS *m/z* 289 $[M+H]^+$.

5,2′,6′-Trihydroxy-7,8-dimethoxyflavone (**4**): yellow amorphous solid ^{1}H and ^{13}C NMR, see Table S3, Supplementary Material; ESIMS *m/z* 331 $[M+H]^+$.

5,2′,6′-Trihydroxy-6,7,8-trimethoxyflavone (**5**): yellow amorphous solid, ^{1}H and ^{13}C NMR, see Table S3, Supplementary Material; ESIMS *m/z* 361 $[M+H]^+$.

5,7,2′-Trihydroxy-8-methoxyflavone (Scutevulin) (**6**): pale yellow amorphous solid, ^{1}H and ^{13}C NMR, see Table S3, Supplementary

Material; ESIMS *m/z* 301 $[M+H]^+$.

5,7,2′-Trihydroxyflavone (**7**): yellow amorphous solid, ^1H and ^{13}C NMR, see Table S3, Supplementary Material; ESIMS *m/z* 271 $[M+H]^+$.

5,7,6′-Trihydroxy-8,2′-dimethoxyflavone (**8**): yellow amorphous solid, ^1H and ^{13}C NMR, see Table S2, Supplementary Material; ESIMS *m/z* 331 $[M+H]^+$.

5,7,2′-Trihydroxy-6-methoxyflavone (Tenaxin II) (**9**): yellow amorphous solid, ^1H and ^{13}C NMR, see Table S4, Supplementary Material; ESIMS *m/z* 301 $[M+H]^+$.

5,6′-Dihydroxy-7,8,2′-trimethoxyflavone (Rivularin) (**10**): yellow amorphous solid, ^1H and ^{13}C NMR, see Table S2, Supplementary Material; ESIMS *m/z* 345 $[M+H]^+$.

Wogonin (**11**): yellow needles, ^1H and ^{13}C NMR, see Table S4, Supplementary Material; ESIMS *m/z* 285 $[M+H]^+$.

5,7-Dihydroxy-6,8-dimethoxyflavone (**12**): yellow amorphous solid, ^1H and ^{13}C NMR, see Table S4, Supplementary Material; ESIMS *m/z* 315 $[M+H]^+$.

Chrysin (**13**): yellow amorphous solid, ^1H and ^{13}C NMR, see Table S4, Supplementary Material; ESIMS *m/z* 255 $[M+H]^+$.

Skullcapflavone II (**14**): yellow amorphous solid, ^1H and ^{13}C NMR, see Table S2, Supplementary Material; ESIMS *m/z* 375 $[M+H]^+$.

Skullcapflavone I (**15**): yellow amorphous solid, ^1H and ^{13}C NMR, see Table S5, Supplementary Material; ESIMS *m/z* 315 $[M+H]^+$.

Oroxylin A (**16**): yellow amorphous solid, ^1H and ^{13}C NMR, see Table S5, Supplementary Material; ESIMS *m/z* 285 $[M+H]^+$.

5,2′-Dihydroxy-6,7,8-trimethoxyflavone (Tenaxin I) (**17**): yellow amorphous solid, ^1H and ^{13}C NMR, see Table S5, Supplementary Material; ESIMS *m/z* 345 $[M+H]^+$.

2.5. Quantification of compounds 11, 13, 14, and 16 in the extract

Stock solutions of compounds **11**, **13**, **14**, and **16** were prepared at concentration of 100 μg/mL in DMSO. The solutions were mixed to yield a stock containing the four analytes at 25 μg/mL each. Serial dilutions with concentrations of 25, 12.5, 3.13, 1.56, and 0.78 μg/mL were prepared from this stock. Concentrations of 100 μg/mL and 50 μg/mL directly from the stock solutions and after a twofold dilution of stock solutions, respectively. Quantification was performed with a Shimadzu HPLC-MS 8030 system equipped with a SunFire® C18 column (3.5 μm, 3.0 ×150 mm) and a electrospray ionization (ESI) interface with a nebulizer gas flow of 3 L/min. Water with 0.1% formic acid (A) and acetonitrile with 0.1% formic acid (B) were used as the mobile phase. The gradient was 35–40% B in 30 min, and retention times were 22.2, 23.7, 24.5, and 25.5 min for **11**, **13**, **14**, and **16**, respectively. Analysis was performed in positive ion mode and with multi reaction monitoring (MRM). The observed transitions in MRM were *m/z* 285 → 168 (quantifier) and 270 (qualifier) for **11** (wogonin), *m/z* 255 → 59, 98 (quantifier), and 153 (qualifier) for **13** (chrysin), *m/z* 375 → 197 (quantifier) and 345 (qualifier) for **14** (skullcapflavone II), *m/z* 285 → 168 (quantifier) and 270 (qualifier) for **16** (oroxylin A).

2.6. Preparation and cultivation of human peripheral lymphocytes

Peripheral blood mononuclear cells (PBMCs) were isolated from the blood of healthy adult donors obtained from the Blood Transfusion Centre (University Medical Centre, Freiburg, Germany). Venous blood was centrifuged on a LymphoPrep® gradient (density: 1.077 g/cm^3, 20 min, 500 *g*, 20 °C; Progen). After centrifugation, cells were wash twice with phosphate-buffered saline (PBS) and subsequently cultured in RPMI 1640 medium supplemented with 10% heat-inactivated fetal calf serum (GE Healthcare Life Sciences), 2 mM L-glutamine, 100 U/mL penicillin, and 100 U/mL streptomycin (all from Life Technologies). The cells were cultured at 37 °C in a humidified incubator with a 5% CO_2/95% air atmosphere.

2.7. T cell proliferation assay

The proliferation of T lymphocytes was determined using CFSE-stainings, as described earlier [8]. Lymphocytes were isolated, washed twice in cold PBS, and resuspended in PBS at concentration of 5 × 10^6 cells/mL. Cells were stained for 10 min at 37 °C with carboxyfluorescein diacetate succinimidyl ester (CFSE; 5 μM: Sigma-Aldrich, St. Louis, MO, USA). The staining was stopped by washing twice with complete medium. Stained lymphocytes (2 ×10^6 cells/mL) were stimulated with anti-human CD3 (clone HIT3a) and anti-human CD28 (clone 28.2) mAbs (each 100 ng/mL; eBioscience) in the presence of either medium, cyclosporine A (CsA; 4.16 μM; Novartis Pharma), camptothecin (CPT; 300 μM; Tocris), or plant extracts/single compounds (concentration range 0.01 – 100 μg/mL) and incubated for 72 h. The negative control remained unstimulated. Flow cytometric analysis of the cell division was performed using a FACSCalibur® instrument (BD Biosciences).

2.8. Determination of apoptosis and necrosis of T cells

Apoptosis and necrosis induction of T lymphocytes were determined via analysis of phosphatidylserine expression of apoptotic cells and, PI permeability of necrotic cells [9]. Lymphocytes were isolated, washed twice in cold PBS, and resuspended in medium at a concentration of 2 × 10^6 cells/mL. Cells were stimulated with anti-human CD3 (clone HIT3a) and anti-human CD28 (clone 28.2) mAbs (each 100 ng/mL; eBioscience) in the presence of either medium, camptothecin (CPT; 300 μM; Tocris), 0.5% Triton-X 100, or plant extracts/single compounds (concentration range 0.01 – 100 μg/mL) and cultivated for 48 h. The negative control remained unstimulated. Cultured cells were washed with PBS and stained with annexin V-FITC using the apoptosis-detection kit (eBioscience) according to the manufacturer's instructions. Propidium iodide (eBioscience) was added, and cells were stained for 15 min at room temperature in the dark. Apoptosis and necrosis rates were determined by flow cytometric analysis using a FACSCalibur® instrument (BD Biosciences).

2.9. Testing of microfractions

The dried microfractions in 96-deepwell plates were redissolved in 25 μL of DMSO by sonication and mixing with a pipette. Of each stock solution, 1 μL was diluted in 100, 300, 900, 2700, 8100, and 24,300 μL of cell suspension, respectively, and tested for inhibition of T-lymphocyte proliferation as described above. Each microfraction was scored based on the number of dilutions showing ≥50% inhibition of proliferation relative to the positive control. Dilutions showing inhibition ≥50% were scored with 1, and those with inhibition ≤50% were considered as inactive and scored with 0.

2.10. In silico predictions

Physicochemical and ADME properties for all isolated compounds were calculated utilizing Percepta® (ACD/Labs, ACD/Percepta Platform, 12.10, 2012).

2.11. Analysis of data

For statistical analysis, data were processed with Microsoft Excel and SPSS software (Version 22.0, IBM, Armonk, USA). Statistical significance was determined with the SPSS software by one-way ANOVA followed by Dunnett's post hoc pairwise comparisons. Values are presented as mean ± standard deviation differences from controls (*$p < 0.05$).

3. Results and discussion

3.1. HPLC-based activity profiling and identification of compounds

The dichloromethane (DCM) extract from the roots of *S. baicalensis* inhibited T-lymphocyte proliferation with an IC_{50} of 12.9 μg/mL (Fig. S1) without concomitant cytotoxicity. Compounds responsible for the activity of the extract were localized with the aid of HPLC-based activity profiling [10]. The extract was submitted to analytical HPLC, and one-minute microfractions were collected and tested. An overlay of the activity profile and the HPLC chromatogram is shown in Fig. 1. Fractions eluted at t_R 14 and 17 min were scored with the highest activity, followed by at the fraction at t_R 10 min. The fraction at t_R 31 min was not considered given that no peak was detected in the chromatogram.

Preparative flash chromatography of the extract on a silica gel column afforded 41 fractions. Compounds that were initially detected in the windows of activity of the activity profile were tracked by HPLC-PDA-MS analysis of these fractions, and purified by semi-preparative RP-HPLC.

The UV spectra of compounds **1–17** exhibited absorption maxima in the region of 260–284 nm, and either a broad shoulder at 300–380 nm or a second absorption maximum between 313 and 340 nm, suggesting the presence of flavonoids [7]. The ESIMS (positive ion mode) showed $[M+H]^+$ adduct ions at *m/z* 255–375 which were in line with the molecular weight of typical flavonoid aglycones. The ^1H NMR spectra of compounds **1–17** exhibited resonances between δ_H 5.50 and 7.00 ppm that were characteristic for protons of ring A, while signals between δ_H 6.00–8.00 ppm were characteristic for the protons on ring B [7]. With exception of **3**, **7**, and **13**, the spectra showed singlets at δ_H 3.50–4.10 ppm (3 H each) that were indicative of one to four aromatic methoxy groups. Flavones **2**, and **4–17**, and flavanones **1** and **3** were readily differentiated based on characteristic ^1H and ^{13}C NMR signals attributable to ring C (Fig. 2; Tables S1-S5). In flavones, H-3 appeared as a singlet at δ_H 6.20–7.10 ppm and C-3 at δ_C 100.0–111.0 ppm, the quaternary carbon C-2 at δ_C 159.0–164.0 ppm, and carbonyl carbon C-4 at δ_C 181.0–184.0 ppm. In flavanones, H-2 appeared at δ_H 5.80 (dd, J = 15.0 and 2.0 Hz), and the diastereotopic methylene protons at C-3 as two dd at δ_H 2.00–4.00 (J = 14.0–18.0 and 2.0–4.0 Hz). The resonances of C-2 and C-3 were at δ_C 40.0 and 71.0 ppm, respectively, and carbonyl carbon C-4 at δ_C 188.8–197.6 ppm.

Complete NMR spectral assignments were achieved by 1D and 2D NMR. The flavones appearing in the active time windows of the activity profile (Fig. 1) were identified as viscidulin III (**2**) [11,12], 5,2′,6′-trihydroxy-6,7,8-trimethoxyflavone (**5**) [13], scutevulin (**6**) [11,14], 5,7,2′-trihydroxyflavone (**7**), 5,7,6′-trihydroxy-8,2′-dimethoxyflavone (**8**) [15], tenaxin II (**9**) [16], rivularin (**10**) [12], wogonin (**11**) [17], 5,7-dihydroxy-6,8-dimethoxyflavone (**12**) [18], chrysin (**13**) [19], skullcapflavone II (**14**) [20], skullcapflavone I (**15**) [21], and oroxylin A (**16**) [22]. Two flavones, 5,2′,6′-trihydroxy-7,8-dimethoxyflavone (**4**) [23] and tenaxin I (**17**) [16], and two flavanones, (*2 S*)−7,2′,6′-trihydroxy-5-methoxyflavanone (**1**) [15] and (*2 S*)−5,7,2′,6′-tetrahydroxyflavanone (**3**) [24], were located in adjacent fractions of the activity profile. The position of hydroxy or methoxy groups at C-5 in flavanones **1** and **3** was established with the aid of UV/Vis shift reagents [7]. In the UV/Vis absorption spectrum of **3**, addition of $AlCl_3$/HCl led to a bathochromic shift of band II (24 nm), whereas no shift was observed in case of **1**. The absolute configuration of flavanones **1** and **3** was determined by ECD (Fig. S2). The ECD spectrum of **1** exhibited positive cotton effects at 223 and 332 nm, and a negative cotton effect at 278 nm. Positive cotton effects at 223 and 325 nm along with a negative cotton effect at 284 nm were observed for **3**. Thus, both compounds had a (*2 S*) configuration [11,24].

All compounds possess an unusual substitution pattern of the B-ring, with an absence of substituents at C-4′, but substituents at C-2′ and C-6′ [7]. Likewise, substituents at C-6 or C-8 are also not very common in flavonoids [6].

3.2. Immunosuppressant activity

All flavonoids in the active time windows of the activity profile (Fig. 1) were flavones with rare substitution patterns. Compounds that

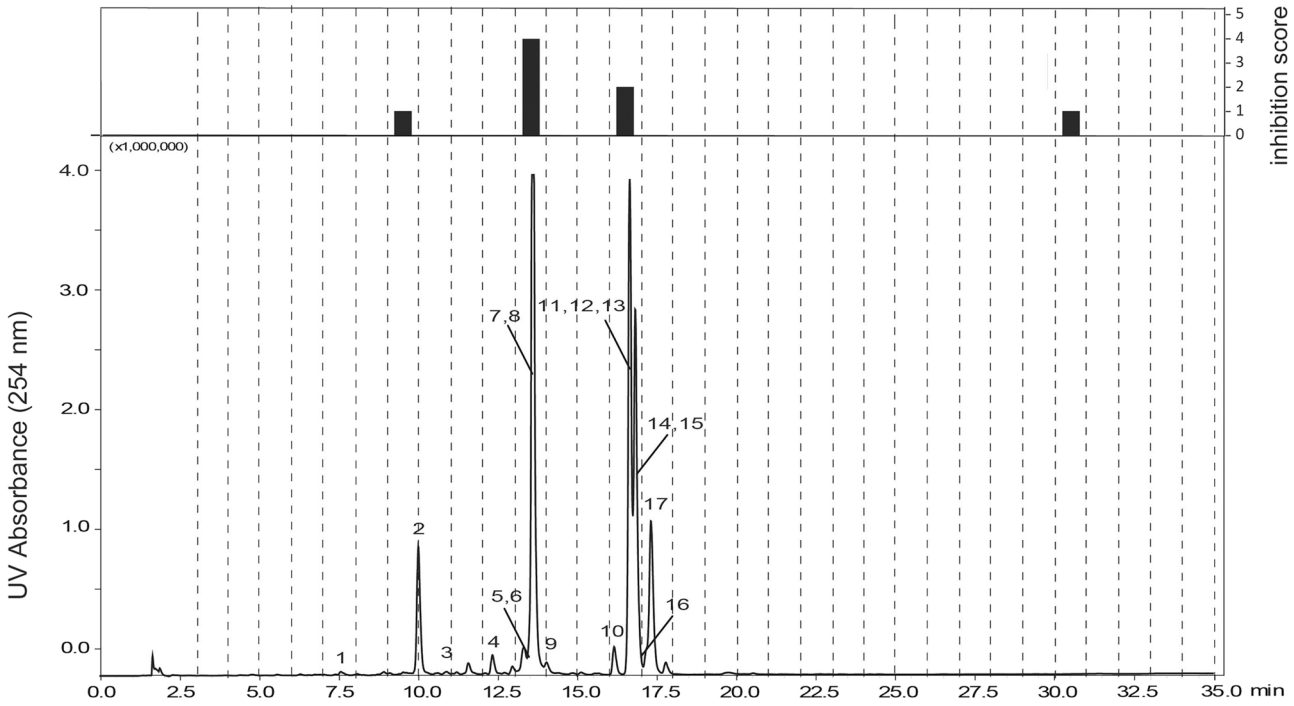

Fig. 1. HPLC chromatogram of the DCM extract of *S. baicalensis* roots (SunFire C18, 3.5 μm, 3.0 ×150 mm i.d.); solvent A: water + 0.1% formic acid, solvent B: acetonitrile + 0.1% formic acid, 20–100% B in 30 min, 100% B for 5 min; flow rate 0.5 mL/min; detection at 254 nm. Microfractions of 1 min each were collected. The bars above the chromatogram show the inhibition scores of microfractions.

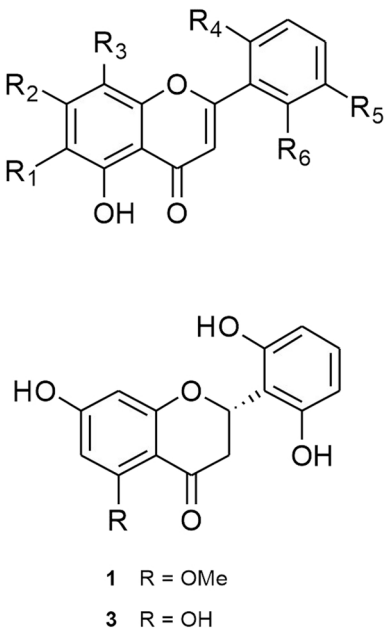

Compound	R_1	R_2	R_3	R_4	R_5	R_6
2	H	OH	OMe	OH	OH	OMe
4	H	OMe	OMe	OH	H	OH
5	OMe	OMe	OMe	OH	H	OH
6	H	OH	OMe	H	H	OH
7	H	OH	H	H	H	OH
8	H	OH	OMe	OH	H	OMe
9	OMe	OH	H	H	H	OH
10	H	OMe	OMe	OH	H	OMe
11	H	OH	OMe	H	H	H
12	OMe	OH	OMe	H	H	H
13	H	OH	H	H	H	H
14	OMe	OMe	OMe	OH	H	OMe
15	H	OMe	OMe	H	H	OH
16	OMe	OH	H	H	H	H
17	OMe	OMe	OMe	H	H	OH

Fig. 2. Structures of isolated compounds.

were available in sufficient amounts (**2**, **4**, and **8–17**) were tested for a concentration-dependent inhibition of T-cell proliferation (Fig. 3, Table 1). FACS analysis of forward and side scatter and cell proliferation were used to assess toxicity and immunosuppressive activity. Compounds **9** and **10** were weakly active, as they showed notable inhibition of T-cell proliferation only at concentrations $\geq$ 25 μg/mL. Compounds **2**, **4**, **8**, and **12** showed intermediate activity, with IC_{50}'s of 55.9, 45.9, 61.6, and 50.2 μM, respectively. High immunosuppressant activity was determined for compounds **11**, **13**, **14**, and **16**, with IC_{50} values of 20.2, 22.2, 12.1, and 39.0 μM, respectively. All compounds showed cytotoxicity at high concentrations. Compounds **1**, **3**, and **5** - **7** could not be tested due to the limited amount of material.

The four most active flavones in the extract were quantified by HPLC-MS-MS in MRM mode, and concentrations of 5.9%, 0.5%, 4.7%, and 3.1%, were found for wogonin (**11**), chrysin (**13**), skullcapflavone (**14**), and oroxylin A (**16**), respectively (Figs. S3 and S4, and Table S6).

The antiproliferative activity of wogonin (**11**) and chrysin (**13**) and the underlying mechanisms have been investigated in different tumor cell lines [25–31], but little evidence has been provided so far for their ability to inhibit primary human immune cell responses. Chrysin reportedly suppresses inflammatory cytokine release of human peripheral blood mononuclear cells [32] and has the potential of diminishing an overactivated immune system [33,34]. Skullcapflavone (**14**) and oroxylin A (**16**) have been studied for their antiproliferative effects in different tumor cell lines [35–38], but not in primary human immune cells.

For a number of structurally diverse flavonoids an inhibition of T-lymphocyte proliferation has been reported. Examples include simple flavones such as luteolin and apigenin [39], methoxyflavones such as hispidulin and nepetin [40], prenylated flavones such as artelastin [41], simple flavonols such as quercetin [42,43] and fisetin [44], prenylated flavonol glycosides such as baohuoside-1 [45,46] and icariin [47], acylated kaempferol derivatives [48], isoflavones such as genistein [49], flavonolignans such as silibinin [50], and delphinidin [51], a widely occurring anthocyanin.

Attempts have been made previously at establishing structure-activity relationships for immunosuppressant flavonoids. For example, a $\Delta^{2,3}$-double bond and a carbonyl group at C-4 were considered as relevant for activity, and flavones decreased T-cell proliferation of murine and human T-cells more strongly than flavonols [39,52]. With respect to substituents at the B-ring, the activity increased from monohydroxy to di- and trihydroxy substituted flavonoids [52]. However, given the highly diverse substitution patterns of the A- and B-rings in our compound series it was not possible to draw firm conclusions on structure-activity relationships.

3.3. Physicochemical and ADME properties of compounds

Given that no clear structure-activity relationship could be derived for our series of flavonoids, the physicochemical and ADME properties, as defined by Lipinski and Veber rules [53–55], were calculated (Table S7). None of the flavonoids exhibited any violations of Lipinski's Rule of Five, with clog P values between 1.73 and 3.11, a molecular weight ranging from 270 to 346 g/M, with 2–4 H donor and 4–8 H acceptor sites, 1–4 rotatable bonds, and 3 rings. ADME profiling showed that predicted solubility ranged from 0.33 mg/mL (soluble) to 0.005 mg/mL (highly insoluble). Caco-2 permeability ranged from 122×10^6 cm/s (highly permeable) to 3×10^6 cm/s (moderately permeable), and a 100% human intestinal absorption (HIA) was predicted for all compounds. Predicted plasma protein binding (PPB) of compounds was moderate to extensive (76–97%), while CNS penetration was weak to absent. Taken together, flavanone **1** had the best overall ADME properties when considering solubility, permeability and plasma protein binding, followed by flavanone **2**, and flavones **4**, **5**, **9** and **10**. The other compounds showed low solubility and extensive plasma protein binding. The most active flavones **11** and **14** both had high predicted permeability and intestinal absorption, but a very low calculated solubility, and strong to extensive plasma protein binding.

4. Conclusion

With the aid of an HPLC-based activity profiling approach the compounds in a lipophilic extract of *S. baicalensis* responsible for a non-cytotoxic inhibition of human T lymphocyte proliferation were located and identified. Skullcapflavone II (**14**) and wogonin (**11**) were the major compounds responsible for the activity of the extract, given their abundance and IC_{50} values, while oroxylin A (**16**) and chrysin (**13**) contributed to a somewhat lesser extent. While the in vitro active compounds showed no Lipinski violations, some unfavorable ADME properties, such as low solubility and high plasma protein binding were

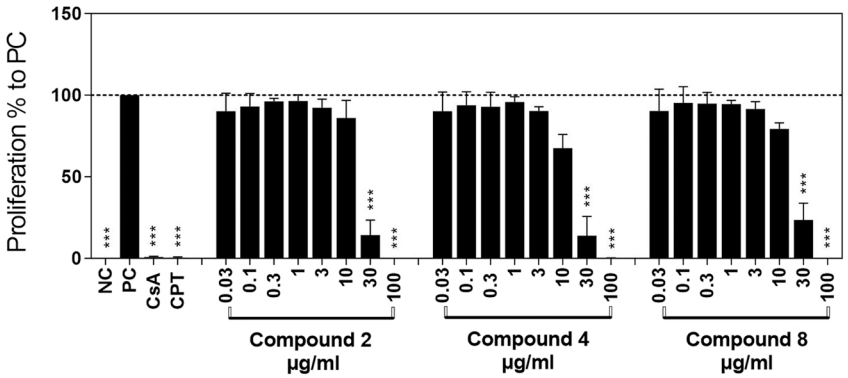

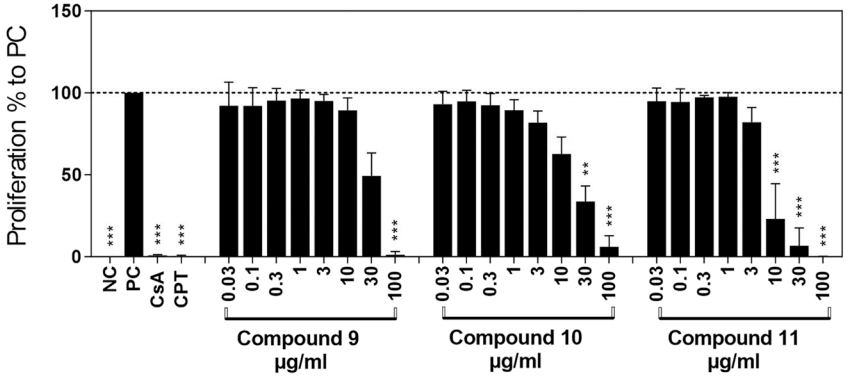

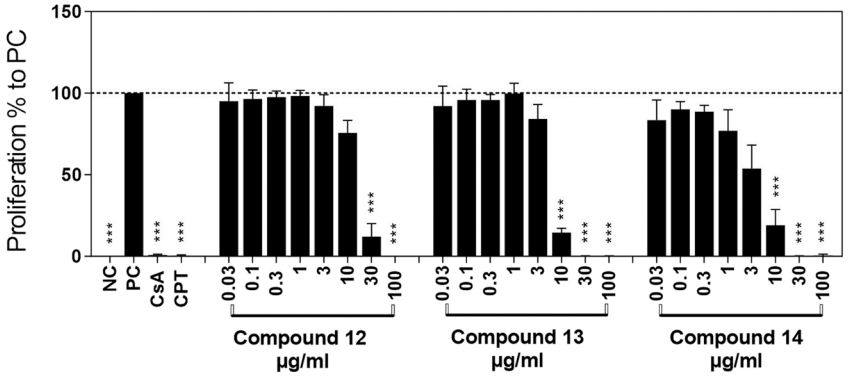

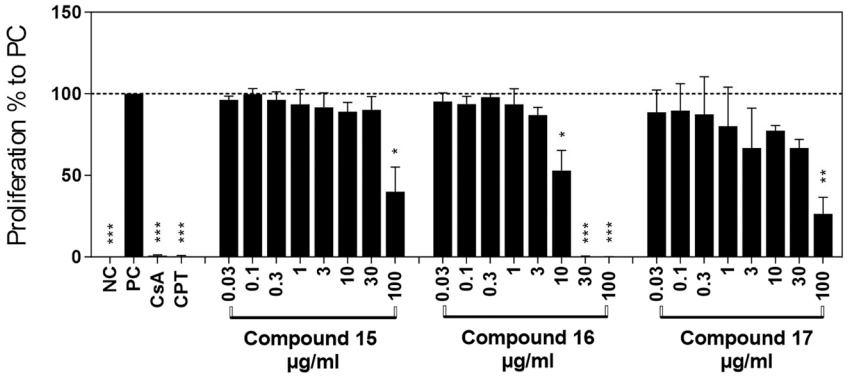

Fig. 3. Inhibitory effects on T-cell proliferation of compounds **2**, **4**, and **8–17**. Data of three independent experiments are depicted as means ± standard deviation in relation to the untreated, stimulated cells as positive control (PC; = 100% ± SD). Non-stimulated cells were used as the negative control (NC), cyclosporine A (CsA; 5 μg/mL) was used as a known inhibitor of T cell proliferation, and camptothecin (CPT; 300 μM) was used as a known inducer of apoptosis. The asterisks represent significant differences from PC (*$p \leq 0.05$, **$p \leq 0.01$, ***$p \leq 0.001$.

Table 1
IC_{50} values calculated for compounds **2**, **4**, and **8–17.**

Compound	IC_{50} value (μg/mL)	IC_{50} (μM)
2	19.3	55.9
4	15.2	45.9
8	20.3	61.6
9	33.1	110.2
10	27.7	80.4
11	5.8	20.2
12	15.8	50.2
13	5.7	22.2
14	4.5	12.1
15	Not calculated	–
16	11.1	39
17	Not calculated	–

indicative of a low oral bioavailability which certainly limits their potential use as pure compounds.

This is in line with previous pharmacokinetic and bioavailability studies on single *Scutellaria* flavonoids. The absolute bioavailability of wogonin (**11**) in beagle dogs was found to be less than 1%, whereby poor solubility and rapid glucuronidation were seen as the major reasons [56]. The oral bioavailability of chrysin (**13**) in rodents was reportedly low due to poor aqueous solubility and significant presystemic elimination [57]. The flavonoid also showed low oral bioavailability in humans, mainly due to extensive phase 2 metabolism (glucuronidation, sulphatation) and efflux of metabolites back into the intestine. The authors estimated a maximal oral bioavailability of 0.02% [58]. Oroxylin A (**16**) also exhibited low oral bioavailability in Beagle dogs, and extensive phase 2 metabolization (mainly sulfatation, less glucuronidation) [59]. Likewise, the oral bioavailability of oroxylin A (**16**) in rats was low, as even with a dose of 360 mg/kg BW the maximum plasma concentrations did not exceed 30 ng/mL [60]. To our knowledge no pharmacokinetic data have been reported for skullcapflavone (**14**).

A further exploration of the immunosuppressive properties may be warranted under the perspective of *S. baicalensis* as a source for phytomedicines. It has been shown that ADME properties of poorly soluble and poorly bioavailable pharmacologically active natural products are significantly improved if they are tested and/or administered in the form of a herbal extract [61–63]. Unfortunately, published bioavailability data for flavonoids in *Scutellaria* extracts are somewhat conflicting. For a standardized *Scutellaria* extract, Fong et al. [64] reported a low oral bioavailability in rats of bacalein, wogonin (**11**) and oroxylin A (**16**). In a similar study, only phase 2 conjugates of bacalein and wogonin (**11**) were detected in rat plasma after oral administration of the extract. Interestingly, free bacalein and wogonin (**11**) were found, together with their phase 2 conjugates, in liver, kidney and lung tissue [65]. Thus, further bioavailability studies would be required to clarify the issue.

Ethics statement

Patients gave their written consent to donate blood for scientific research. All experiments conducted on human material were approved by the Ethics Committee of the University of Freiburg (55/14).

CRediT authorship contribution statement

NS performed isolation, structure elucidation, and *in silico* calculation. SD and AM performed the bioassays and analyzed the data. JK performed the initial microfractionation. OD assisted in NMR and ECD analysis. CG and MH designed and supervised the project. NS wrote the draft manuscript which was finalized by MH and CG. All authors read and approved the final manuscript.

Declaration of Competing Interest

The authors declare that they have no known competing financial interests or personal relationships that could have appeared to influence the work reported in this paper.

Acknowledgements

NS thanks the Indonesia Endowment Fund for Education (LPDP) for a fellowship. C.G. is supported by PRIAM-BS (Verein Stiftungsprofessur für Integrative und Anthroposophische Medizin an der Universität Basel). Technical assistance of Orlando Fertig is gratefully acknowledged. Parts of this work was presented at the 67th International Congress and Annual Meeting of the Society for Medicinal Plant and Natural Product Research, Innsbruck; Austria, September 1–5, 2019, as a poster contribution, and the conference abstract published in *Planta Medica* (doi: 10.1055/s-0039-3399888).

Appendix A. Supporting information

Supplementary data associated with this article can be found in the online version at doi:10.1016/j.biopha.2021.112326.

References

[1] F.R. Santori, The immune system as self-centered network of lymphocytes, Immunol. Lett. 166 (2015) 109–116.
[2] U. Khan, H. Ghazanfar, T lymphocytes and autoimmunity, Int. Rev. Cell Mol. Biol. 342 (2018) 125–168.
[3] J.K. Reinhardt, A.M. Klemd, O. Danton, M.D. Mieri, M. Smiesko, R. Huber, T. Bürgi, C. Gründemann, M. Hamburger, Sesquiterpene lactones from *Artemisia argyi*: absolute configuration and immunosuppressant activity, J. Nat. Prod. 82 (2019) 1424–1433.
[4] A.M. Zimmermann-Klemd, J.K. Reinhardt, A. Morath, W.W. Schamel, P. Steinberger, J. Leitner, R. Huber, M. Hamburger, C. Gründemann, Immunosuppressive activity of *Artemisia argyi* extract and isolated compounds, Front. Pharmacol. 11 (2020) 1–13.
[5] W. Tang, G. Eisenbrand, Handbook of Chinese Medicinal Plants, Vol. 2, Wiley-VCH, Weinheim, 2011.
[6] Z.-L. Wang, S. Wang, Y. Kuang, Z.-M. Hu, X. Qiao, M. Ye, A comprehensive review on phytochemistry, pharmacology, and flavonoid biosynthesis of *Scutellaria baicalensis*, Pharm. Biol. 56 (2018) 465–484.
[7] J.B. Harborne, T.J. Mabry, H. Mabry, The Flavonoids, Academic Press, New York, 1975.
[8] C.R. Parish, M.H. Glidden, B.J.C. Quah, H.S. Warren, 2009. Current Protocols in Immunology, 4.9.1–4.9.13.
[9] I. Vermes, C. Haanen, C. Reutelingsperger, Flow cytometry of apoptotic cell death, J. Immunol. Methods 243 (2000) 167–190.
[10] O. Potterat, M. Hamburger, Combined use of extract libraries and HPLC-based activity profiling for lead discovery: potential, challenges, and practical considerations, Planta Med 80 (2014) 1171–1181.
[11] T. Tomimori, Y. Miyaichi, Y. Imoto, H. Kizu, C. Suzuki, Studies on the constituents of *Scutellaria* species. IV. On the flavonoid constituents of the root of *Scutellaria baicalensis* George, Yakugaku Zasshi 104 (1984) 529–534.
[12] Y.-Y. Zhang, Y.-Z. Guo, M. Onda, K. Hashimoto, Y. Ikeya, M. Okada, M. Maruno, Four flavonoids from *Scutellaria baicalensis*, Phytochemistry 35 (1994) 511–514.
[13] Y. Kikuchi, Y. Miyaichi, Y. Yamaguchi, H. Kizu, T. Tomimori, K. Vetschera, Studies on the constituents of *Scutellaria* species. XIV. On the constituents of the root and the leaves of *Scutellaria alpina* L, Chem. Pharm. Bull. 39 (1991) 199–201.
[14] V.M. Malikov, M.P. Yuldashev, Phenolic compounds of plants of the *Scutellaria* L. genus. Distribution, structure, and properties, Chem. Nat. Compd. 38 (2002) 358–406.
[15] T. Tomimori, Y. Miyaichi, Y. Imoto, H. Kizu, Y. Tanabe, Studies on the constituents of *Scutellaria* species. III. On the flavonoid constituents of the root of *Scutellaria baicalensis* Georgi, Yakugaku Zasshi 104 (1984) 524–528.
[16] T. Tomimori, Y. Miyaichi, Y. Imoto, H. Kizu, Y. Tanabe, Studies on the constituents of *Scutellaria* species. II. On the flavonoid constituents of the root of *Scutellaria baicalensis* Georgi, Yakugaku Zasshi 103 (1983) 607–611.
[17] T. Li, T. Weng, J. Wang, Z. Wei, L. Zhao, Z. Li, A practical and efficient approach to the preparation of bioactive natural product wogonin, Org. Process Res. Dev. 21 (2017) 171–176.
[18] T. Horie, Y. Kawamura, H. Yamamoto, T. Kitou, K. Yamashita, Synthesis of 5,8-dihydroxy-6,7-dimethoxyflavones and revised structures for some natural flavones, Phytochemistry 39 (1995) 1201–1210.
[19] S. Takagi, M. Yamaki, K. Inoue, Studies on the water-soluble constituents of the roots of *Scutellaria baicalensis* Georgi (Wogon), Yakugaku Zasshi 100 (1980) 1220–1224.
[20] M. Takido, M. Aimi, S. Takahashi, S. Yamanouchi, H. Torii, S. Dohi, Studies on the constituents in the water extracts of crude drugs. I. On the roots of *Scutellaria baicalensis* Georgi (Wogon), Yakugaku Zasshi 95 (1975) 108–113.

[21] T. Horie, M. Tsukayama, M. Masumura, M. Nakayama, S. Hayashi, The synthesis of 5,2′-dihydroxy-6,8-dimethoxyflavone and its isomers: a revised structure of skullcapflavone I, Bull. Chem. Soc. Jpn. 52 (1979) 2950–2952.

[22] W.-H. Huang, P.-Y. Chien, C.-H. Yang, A.-R. Lee, Novel synthesis of flavonoids of *Scutellaria baicalensis* Georgi, Chem. Pharm. Bull. 51 (2003) 339–340.

[23] I.I. Chemesova, M. Iinuma, A.L. Budanstev, Investigation of the flavonoid composition of *Scutellaria adenostegia*, Chem. Nat. Compd. 29 (1993) 133–134.

[24] M. Kubo, Y. Kimura, T. Odani, T. Tani, K. Namba, Studies on Scutellariae radix, Planta Med. 43 (1981) 194–201.

[25] Y. Wang, S. Chen, S. Sun, G. Liu, L. Chen, Y. Xia, J. Cui, W. Wang, X. Jiang, L. Zhang, Y. Zhu, Y. Zou, B. Shi, Wogonin induces apoptosis and reverses sunitinib resistance of renal cell carcinoma cells via inhibiting CDK4-RB pathway, Front. Pharmacol. 11 (2020) 1152.

[26] M. Hong, M.M. Almutairi, S. Li, J. Li, Wogonin inhibits cell cycle progression by activating the glycogen synthase kinase-3 beta in hepatocellular carcinoma, Phytomedicine 68 (2020), 153174.

[27] S.-J. Wang, J.-K. Zhao, S. Ren, W.-W. Sun, W.-J. Zhang, J.-N. Zhang, Wogonin affects proliferation and the energy metabolism of SGC-7901 and A549 cells, Exp. Ther. Med. 17 (2019) 911–918.

[28] M. Ali, M. Bonay, V. Vanhee, S. Vinit, T.B. Deramaudt, Comparative effectiveness of 4 natural and chemical activators of Nrf2 on inflammation, oxidative stress, macrophage polarization, and bactericidal activity in an in vitro macrophage infection model, PLoS One 15 (2020), e0234484.

[29] J.Y. Lee, W. Park, Anti-inflammatory effect of wogonin on RAW 264.7 mouse macrophages induced with polyinosinic-polycytidylic acid, Molecules 20 (2015) 6888–6900.

[30] A.P.B. Lima, T.C. Almeida, T.M.B. Barros, L.C.M. Rocha, C.C.M. Garcia, G.N. da Silva, Toxicogenetic and antiproliferative effects of chrysin in urinary bladder cancer cells, Mutagenesis 35 (2020) 361–371.

[31] A. Sassi, I.M. Bzéouich, N. Mustapha, M. Maatouk, K. Ghedira, L. Chekir-Ghedira, Immunomodulatory potential of hesperetic and chrysin through the cellular and humoral response, Eur. J. Pharmacol. 812 (2017) 91–96.

[32] S. Touzani, W. Embaslat, H. Imtara, A. Kmail, S. Kadan, H. Zaid, I. ElArabi, L. Badiaa, B. Saad, In vitro evaluation of the potential use of propolis as a multitarget therapeutic product: physicochemical properties, chemical composition, and immunomodulatory, antibacterial, and anticancer properties, Biomed. Res. Int. 2019 (2019), 4836378.

[33] H.-J. Li, N.-L. Wu, C.-M. Pu, C.-Y. Hsiao, D.-C. Chang, C.-F. Hung, Chrysin alleviates imiquimod-induced psoriasis-like skin inflammation and reduces the release of CCL20 and antimicrobial peptides, Sci. Rep. 10 (2020) 2932.

[34] M. Zeinali, S.A. Rezaee, H. Hosseinzadeh, An overview on immunoregulatory and anti-inflammatory properties of chrysin and flavonoids substances, Biomed. Pharmacother. 92 (2017) 998–1009.

[35] J. Cui, H. Li, Y. Wang, T. Tian, C. Liu, Y. Wang, S. Sun, B. Feng, Skullcapflavone I has a potent anti-pancreatic cancer activity by targeting miR-23a, BioFactors 46 (2020) 821–830.

[36] Y. Yang, R. An, T. Feng, X. Qin, J. Zhang, Y. Bo, B. Niu, Skullcapflavone I suppresses proliferation of human lung cancer cells via down-regulating microRNA-21, Exp. Mol. Pathol. 110 (2019), 104285.

[37] L. Wei, Y. Zhou, C. Qiao, T. Ni, Z. Li, Q. You, Q. Guo, N. Lu, Oroxylin A inhibits glycolysis-dependent proliferation of human breast cancer via promoting SIRT3-mediated SOD2 transcription and HIF1α destabilization, Cell Death Dis. 6 (2015), e1714.

[38] J. Yao, R. Hu, J. Sun, B. Lin, L. Zhao, Y. Sha, B. Zhu, Q.-D. You, T. Yan, Q.-L. Guo, Oroxylin A prevents inflammation-related tumor through down-regulation of inflammatory gene expression by inhibiting NF-kB signaling, Mol. Carcinog. 53 (2014) 145–158.

[39] R. Verbeek, A.C. Plomp, E.A.F. van Tol, J.M. van Noort, The flavones luteolin and apigenin inhibit in vitro antigen-specific proliferation and interferon-gamma production by murine and human autoimmune T cells, Biochem. Pharm. 68 (2004) 621–629.

[40] P. Thitilertdecha, V. Tantithavorn, P. Poungpairoj, N. Onlamoon, Determination of suppressive effect on human T-cell activation by hispidulin, nepetin, and vanilic acid, Immunopharmacol. Immunotoxicol. 41 (2019) 591–598.

[41] F. Cerqueira, A. Cordeiro-Da-Silva, N. Araujo, H. Cidade, A. Kijjoa, M.S. J. Nascimento, Inhibition of lymphocyte proliferation by prenylated flavones: artelastin as a potent inhibitor, Life Sci. 73 (2003) 2321–2334.

[42] Z. Sternberg, K. Chadha, A. Lieberman, D. Hojnacki, A. Drake, P. Zamboni, P. Rocco, E. Grazioli, B. Weinstock-Guttman, F. Munschauer, Quercetin and interferon-β modulate immune response(s) in peripheral blood mononuclear cells isolated from multiple sclerosis patients, J. Neuroimmunol. 205 (2008) 142–147.

[43] S. Hushmendy, L. Jayakumar, A.B. Hahn, D. Bhoiwala, D.L. Bhoiwala, D. R. Crawford, Select phytochemicals suppress human T-lymphocytes and mouse splenocytes suggesting their use in autoimmunity and transplantation, Nutr. Res. 29 (2009) 568–578.

[44] B. Song, S. Guan, J. Lu, Z. Chen, G. Huang, G. Li, Y. Xiong, S. Zhang, Z. Yue, X. Deng, Suppressive effects of fisetin on mice T lymphocytes in vitro and in vivo, J. Surg. Res. 185 (2013) 399–409.

[45] A. Ma, S. Qi, D. Xu, X. Zhang, P. Daloze, H. Chen, Baohuoside-1, a novel immunosuppressive molecule, inhibits lymphocyte activation in vitro and in vivo, Transplantation 78 (2004) 831–838.

[46] A. Ma, S. Qi, D. Xu, P. Daloze, H. Chen, Baohuoside-1 inhibits activated T cell proliferation at G_1 -S phase transition, Transpl. Immunol. 15 (2005) 55–62.

[47] R. Shen, W. Deng, C. Li, G. Zeng, A natural flavonoid glucoside icariin inhibits Th1 and Th17 cell differentiation and ameliorates experimental autoimmune encephalomyelitis, Int. Immunopharmacol. 24 (2015) 224–231.

[48] Y.-C. Kuo, C.-K. Lu, L.-W. Huang, Y.-H. Kuo, C. Chang, F.-L. Hsu, T.-H. Lee, Inhibitory effects of acylated kaempferol glycosides from the leaves of *Cinnamomum kotoense* on the proliferation of human peripheral blood mononuclear cells, Planta Med. 71 (2005) 412–415.

[49] F. Traganos, B. Ardelt, N. Halko, S. Bruno, Z. Darzynkiewicz, Effects of genistein on the growth and cell cycle progression of normal human lymphocytes and human leukemic MOLT-4 and HL-60 cells, Cancer Res. 52 (1992) 6200–6208.

[50] J. McClure, E.S. Lovelace, S. Elahi, N.J. Maurice, J. Wagoner, J. Dragavon, J. E. Mittler, Z. Kraft, L. Stamatatos, H. Horton, S.C. De Rosa, R.W. Coombs, S. J. Polyak, Silibinin inhibits HIV-1 infection by reducing cellular activation and proliferation, PLoS One 7 (2012), e41832.

[51] O. Dayoub, S.L. Lay, R. Soleti, N. Clere, G. Hilairet, S. Dubois, F. Gagnadoux, J. Boursier, M.C. Martinez, R. Andriantsitohaina, Estrogen receptor α/HDAC/NFAT axis for delphinidin effects on proliferation and differentiation of T lymphocytes from patients with cardiovascular risks, Sci. Rep. 7 (2017) 1–17.

[52] C.-J. Kim, S.K. Cho, Pharmacological activities of flavonoids (III). Structure-activity relationships of flavonoids in immunosuppression, Arch. Pharm. Res. 14 (1991) 147–159.

[53] C.A. Lipinski, F. Lombardo, B.W. Dominy, P.J. Feeney, Experimental and computational approaches to estimate solubility and permeability in drug discovery and development settings, Adv. Drug Deliv. Rev. 23 (1997) 3–25.

[54] C.A. Lipinski, F. Lombardo, B.W. Dominy, P.J. Feeney, Experimental and computational approaches to estimate solubility and permeability in drug discovery and development settings, Adv. Drug Deliv. Rev. 46 (2001) 3–26.

[55] D.F. Veber, S.R. Johnson, H.-Y. Cheng, B.R. Smith, K.W. Ward, K.D. Kopple, Molecular properties that influence the oral bioavailability of drug candidates, J. Med. Chem. 45 (2002) 2615–2623.

[56] N. Zhu, J.-C. Li, J.-X. Zhu, X. Wang, J. Zhang, Characterization and bioavailability of wogonin by different administration routes in beagles, Med. Sci. Monit. 22 (2016) 3737–3745.

[57] V. Mohos, E. Fliszár-Nyúl, G. Schilli, C. Hetényi, B. Lemli, S. Kunsági-Máté, B. Bognár, M. Poór, Interaction of chrysin and its main conjugated metabolites chrysin-7-sulfate and chrysin-7-glucuronide with serum albumin, Int. J. Mol. Sci. 19 (2018) 4073.

[58] T. Walle, Y. Otake, J.A. Brubaker, U.K. Walle, P.V. Halushka, Disposition and metabolism of the flavonoid chrysin in normal volunteers, Br. J. Clin. Pharm. 51 (2001) 143–146.

[59] G. Ren, H. Chen, M. Zhang, N. Yang, H. Yang, C. Xu, J. Li, C. Ning, Z. Song, S. Zhou, S. Zhang, X. Wang, Y. Lu, N. Li, Y. Zhang, X. Chen, D. Zhao, Determination of oroxylin A, oroxylin A 7-*O*-glucuronide, and oroxylin A sodium sulfonate in beagle dogs by using UHPLC MS/MS application in a pharmacokinetic study, J. Sep. Sci. 43 (2020) 2290–2300.

[60] G. Ren, H. Chen, M. Zhang, N. Yang, H. Yang, C. Xu, J. Li, C. Ning, Z. Song, S. Zhou, Y. Bian, Y. Lu, N. Li, Y. Zhang, X. Chen, D. Zhao, Pharmacokinetics, tissue distribution and excretion study of oroxylin A, oroxylin A 7-O-glucuronide and oroxylin A sodium sulfonate in rats after administration of oroxylin A, Fitoterapia 142 (2020), 104480.

[61] A. Nahrstedt, V. Butterweck, Lessons learned from herbal medicinal products: the example of St. John's Wort, J. Nat. Prod. 73 (2010) 1015–1021.

[62] C. Oberthür, C. Heineman, P. Elsner, E. Benfeldt, M. Hamburger, A comparative study on the skin penetration of pure tryptanthrin and tryptanthrin in *Isatis tinctoria* extract by dermal microdialysis coupled with isotope dilution ESI-LC-MS, Planta Med. 69 (2003) 385–389.

[63] J. Gertsch, Botanical drugs, synergy, and network pharmacology: forth and back to intelligent mixtures, Planta Med. 77 (2011) 1086–1098.

[64] S.Y.K. Fong, Y.C. Wong, Z. Zuo, Development of a SPE-LC/MS/MS method for simultaneous quantification of baicalein, wogonin, oroxylin A and their glucuronides baicalin, wogonoside and oroxyloside in rats and its application to brain uptake and plasma pharmacokinetic studies, J. Pharm. Biomed. Anal. 97 (2014) 9–23.

[65] Y.-C. Hou, S.-P. Lin, S.-Y. Tsai, M.-H. Ko, Y.-C. Chang, P.-D.L. Chao, Flavonoid pharmacokinetics and tissue distribution after repeated dosing of the roots of *Scutellaria baicalensis* in rats, Planta Med. 77 (2011) 455–460.